Elucidation of the mechanism of phase transition in zinc-formate framework templated by diammonium cation – the structural, phonon and dielectric studies

Aneta Ciupa-Litwa[a*], Jan Janczak[a], Paulina Peksa[b], Adam Sieradzki[b]

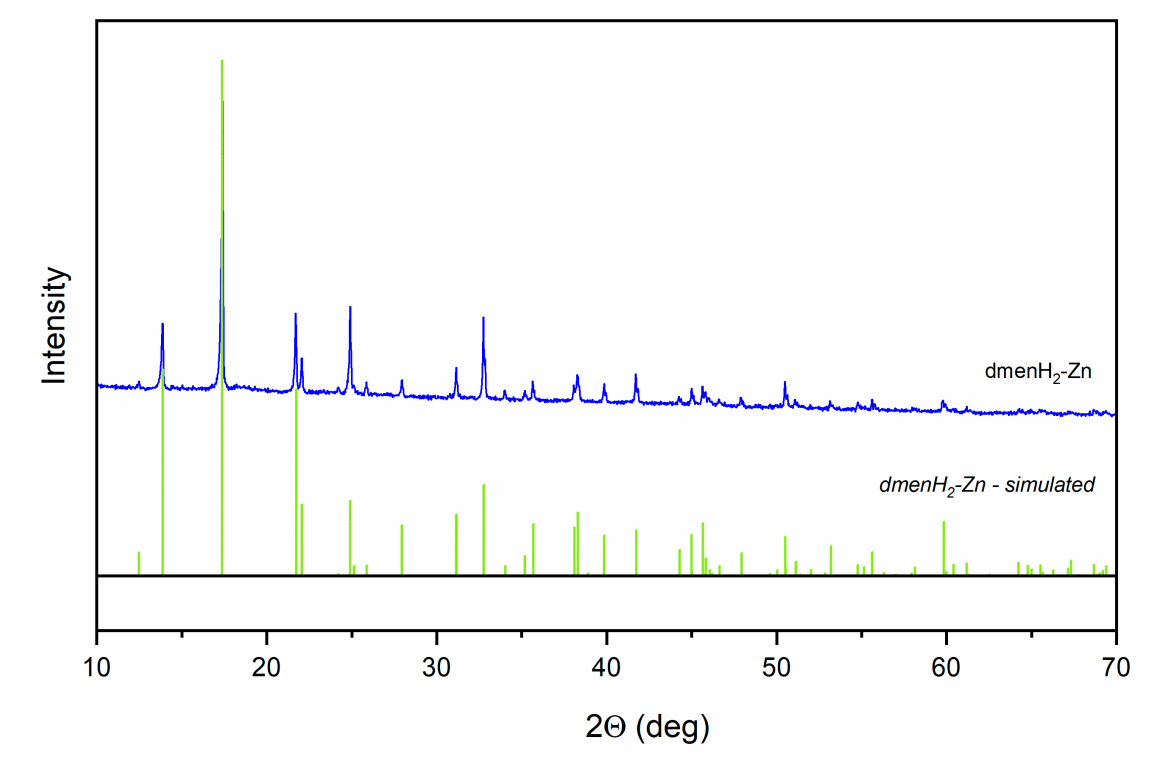

Figure S1. Powder XRD patterns for the as-prepared bulk sample of dmenH$_2$-Zn with the calculated one based on the single crystal structures at 300 K.

Trigonal (RT) Monoclinic (low temp.)

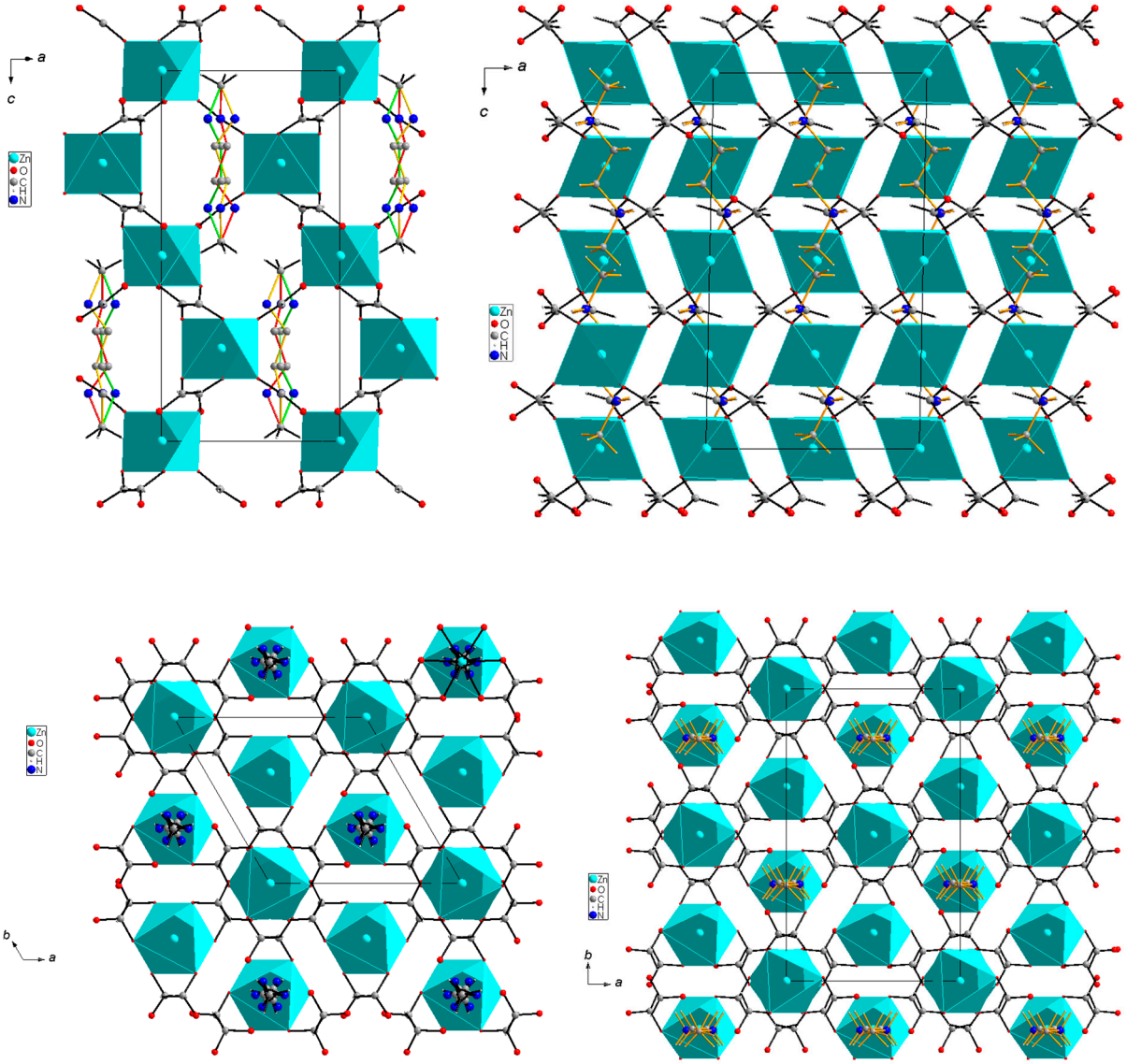

(a) (b)

Figure S2. Projection of the anionic pseudo-perovskite Zn-formate framework together with the $dmenH_2^{2+}$ counter-ions in the cavities in the RT trigonal (a) and LT monoclinic (b) modifications viewed along the *b* and *c* axis.

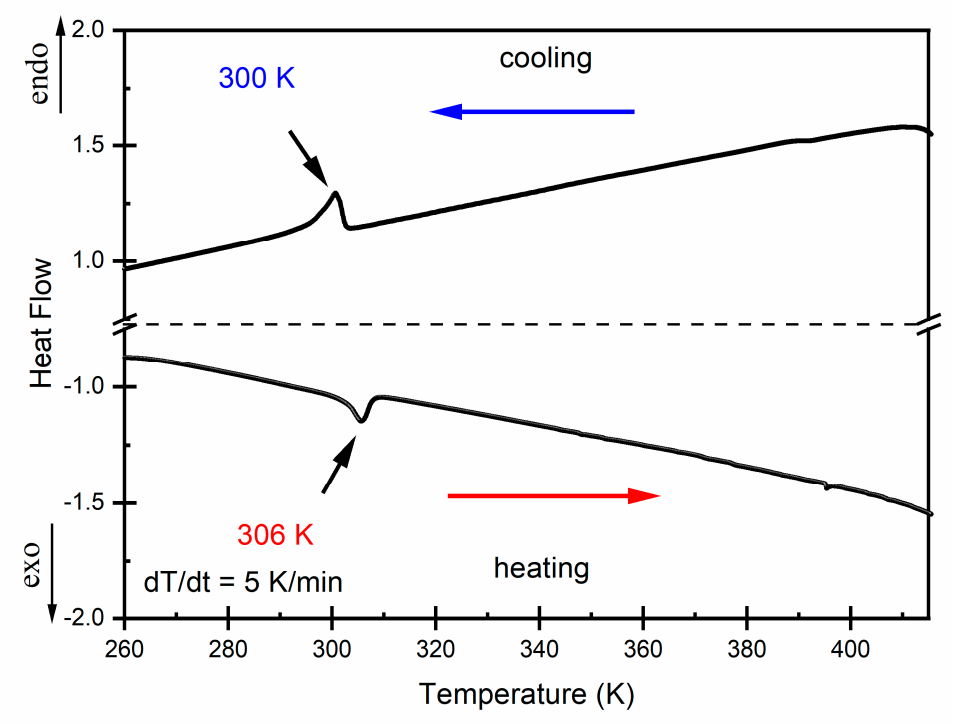

Figure S3. DSC data for dmenH_2-Zn between 260K and 420K for cooling and heating run.

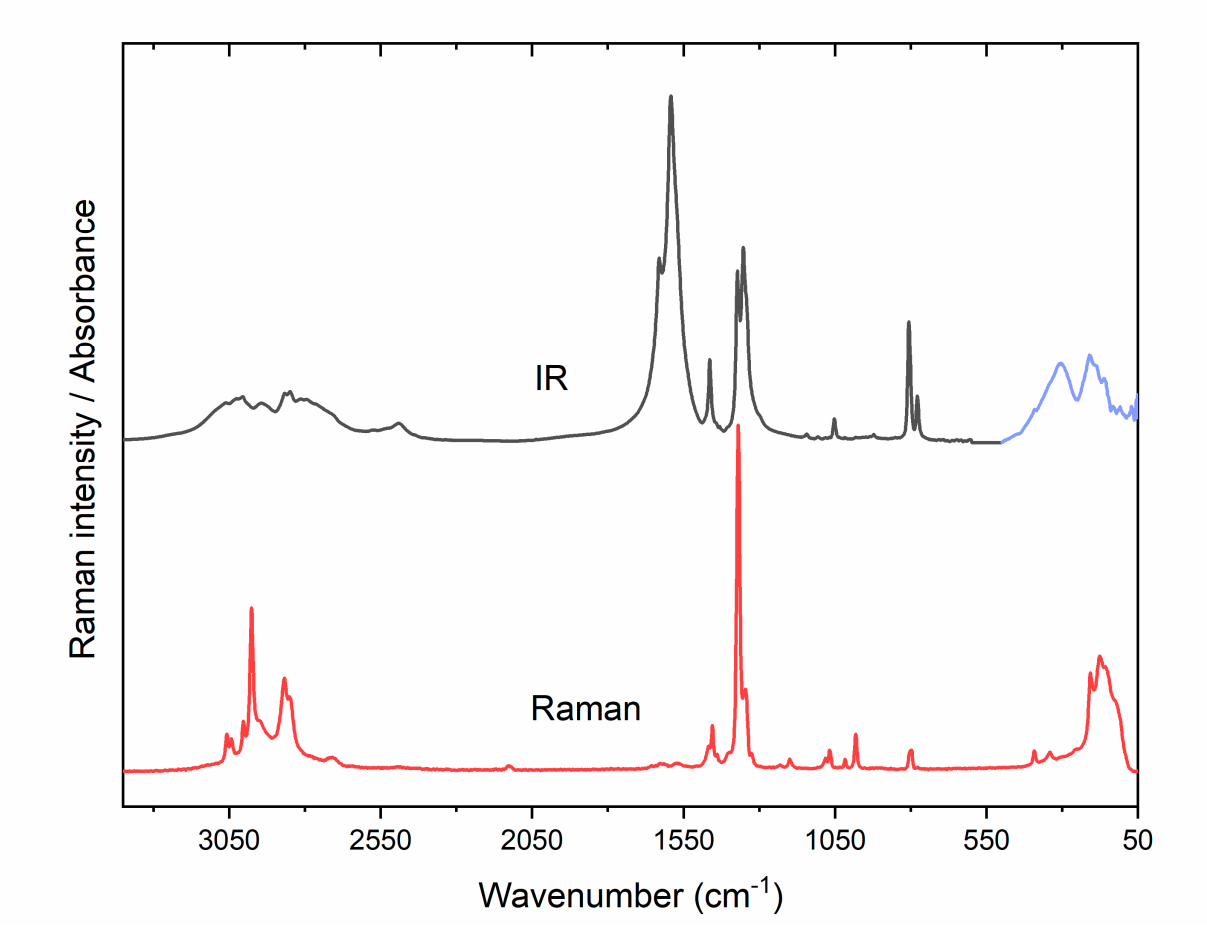

Figure S4. The polycrystalline IR and Raman spectra of the studied dmenH_2-Zn compound.

Table S1. Factor group analysis for **dmenH$_2$-Zn**. The number of nonequivalent $HCOO^-$ ions is six and divalent zinc ions (Zn^{2+}) is two, therefore, the total number of vibrational modes for formate ion is six time larger and for metal ions two times larger than presented by the correlation diagram.[a]

Ion	Vibration	Free ion symmetry	Site symmetry	Factor group symmetry
		C_{2v}	**C_1**	**C_{2h}**
$HCOO^-$	ν_1, ν_2 or ν_3	A_1	A	$A_u + A_g + B_g + B_u$
	ν_4, ν_5 or ν_6	B_1	A	$A_u + A_g + B_g + B_u$
	T’	$A_1 + B_1 + B_2$	3A	$3A_u + 3A_g + 3B_g + 3B_u$
	L	$A_2 + B_1 + B_2$	3A	$3A_u + 3A_g + 3B_g + 3B_u$
		C_1	**C_1**	**C_{2h}**
$dmenH_2^{2+}$	$\nu_s(CH_3)$	2A	2A	$2A_u + 2A_g + 2B_g + 2B_u$
	$\nu_{as}(CH_3)$	2A	2A	$2A_u + 2A_g + 2B_g + 2B_u$
	$\delta_s(CH_3)$	2A	2A	$2A_u + 2A_g + 2B_g + 2B_u$
	$\delta_{as}(CH_3)$	2A	2A	$2A_u + 2A_g + 2B_g + 2B_u$
	$\tau(CH_3)$	2A	2A	$2A_u + 2A_g + 2B_g + 2B_u$
	$\rho(CH_3)$	2A	2A	$2A_u + 2A_g + 2B_g + 2B_u$
	$\omega(CH_3)$	2A	2A	$2A_u + 2A_g + 2B_g + 2B_u$
	$\nu_s(CH_2)$	2A	2A	$2A_u + 2A_g + 2B_g + 2B_u$
	$\nu_{as}(CH_2)$	2A	2A	$2A_u + 2A_g + 2B_g + 2B_u$
	$\delta_s(CH_2)$	2A	2A	$2A_u + 2A_g + 2B_g + 2B_u$
	$\delta_{as}(CH_2)$	2A	2A	$2A_u + 2A_g + 2B_g + 2B_u$
	$\tau(CH_2)$	2A	2A	$2A_u + 2A_g + 2B_g + 2B_u$
	$\rho(CH_2)$	2A	2A	$2A_u + 2A_g + 2B_g + 2B_u$
	$\omega(CH_2)$	2A	2A	$2A_u + 2A_g + 2B_g + 2B_u$
	$\nu_s(CNC)$	2A	2A	$2A_u + 2A_g + 2B_g + 2B_u$
	$\nu_{as}(CNC)$	2A	2A	$2A_u + 2A_g + 2B_g + 2B_u$

	δ_s(CNC)	2A	2A	$2A_u + 2A_g + 2B_g + 2B_u$
	δ_{as}(CNC)	A	A	$2A_u + 2A_g + 2B_g + 2B_u$
	ν(CC)	2A	2A	$A_u + A_g + B_g + B_u$
	ν(NCC)	2A	2A	$2A_u + 2A_g + 2B_g + 2B_u$
	δ(NCC)	2A	2A	$2A_u + 2A_g + 2B_g + 2B_u$
	τ(NCCN)	A	A	$A_u + A_g + B_g + B_u$
	$\nu_s(NH_2)$	2A	2A	$2A_u + 2A_g + 2B_g + 2B_u$
	$\nu_{as}(NH_2)$	2A	2A	$2A_u + 2A_g + 2B_g + 2B_u$
	$\delta(NH_2)$	2A	2A	$2A_u + 2A_g + 2B_g + 2B_u$
	$\tau(NH_2)$	2A	2A	$2A_u + 2A_g + 2B_g + 2B_u$
	$\rho(NH_2)$	2A	2A	$2A_u + 2A_g + 2B_g + 2B_u$
	$\omega(NH_2)$	2A	2A	$2A_u + 2A_g + 2B_g + 2B_u$
	T’	3A	3A	$3A_u + 3A_g + 3B_g + 3B_u$
	L	3A	3A	$3A_u + 3A_g + 3B_g + 3B_u$

Zn^{2+}	C_1	C_{2h}
	3A	$3A_u + 3A_g + 3B_g + 3B_u$

[a]Key: ν_s, ν_{as}, δ_s, δ_{as}, ρ, τ, ω denote symmetric stretching, asymmetric, stretching, symmetric bending, asymmetric bending, rocking, twisting and wagging vibrations. T’ and L denote translations and librations.

Table S2. The assignment of the bands (in cm^{-1}) of dmenH_2-Zn.

Raman	IR		Assignment
	400 K	100 K	
	3095b,m	3094b,m	$\nu(NH_2)$
3057w	3060m	3058m	$\nu(NH_2)$
3043m			$\nu(CH_3)$
	3029m	3023b,m	$\nu(NH_2)$
3003m	3004m	3003m, 2993sh	$\nu(CH_3)$
2976s			$\nu(CH_2)$
2948m	2946m	2941m	$\nu(CH_2)$
	2923m	2927m	$\nu(CH_2)$
		2881m	ν_1(HCOO) + $\nu(CH_3)$
2868s	2864m	2862m	ν_1(HCOO) + $\nu(CH_3)$ + $\nu(CH_2)$

2849s	2848m	2848m	$\nu(CH_3) + \nu(CH_2)$
	2815b,m	2814m	$\nu(CH_3) + \nu(CH_2)$
	2793b,m	2792m	$\nu(CH_3) + \nu(CH_2)$
		2771m	$\nu(CH_3) + 2\nu_2(HCOO)$
		2747m	$\nu(CH_3) + 2\nu_2(HCOO)$
2709b,w	2710b,m	2713w	$\nu(CH_3) + \nu(CH_2)$
		2701w	$\nu(CH_3) + 2\nu_2(HCOO)$
		2666w	$\nu(CH_3) + 2\nu_2(HCOO)$
		2615vw	$\nu(CH_3) + 2\nu_2(HCOO)$
		2606vw	$\nu(CH_3) + 2\nu_2(HCOO)$
	2568b,w	2578w	$\nu(CH_3) + 2\nu_2(HCOO)$
		2534w	$\nu(CH_3) + 2\nu_2(HCOO)$
		2501m	$\nu(CH_3) + 2\nu_2(HCOO)$
	2484b,m	2492m	$\nu(CH_3) + 2\nu_2(HCOO)$
		2436w	$\nu(CH_3) + 2\nu_2(HCOO)$
		2404w	$\nu(CH_3) + 2\nu_2(HCOO)$
1625vw	1627s	1640s, 1636s	$\nu_4(HCOO)$
	1591vs	1599vs, 1587vs	$\nu_4(HCOO)$
1572vw	1574sh	1576sh	$\nu_4(HCOO)$
		1537w,sh	$\delta(NH_2)$
		1475w	$\delta(CH_3) + \delta(CH_2)$
1465m	1462m	1463m	$\delta(CH_3) + \delta(CH_2)$
1454m		1455w	$\delta(CH_3) + \delta(CH_2)$
1439w		1439w	$\delta(CH_3) + \delta(CH_2)$
	1430b,vw	1433w	$\delta(CH_3) + \delta(CH_2)$
		1428w	$\delta(CH_3) + \delta(CH_2)$
1399m		1402vw	$\nu_5(HCOO)$
1369vs	1371m	1375s, 1368m	$\nu_5(HCOO)$
	1367m	1364m	$\nu_2(HCOO) + \omega(CH_2)$
1350m	1353m	1353m	$\nu_2(HCOO) + \omega(CH_2)$
1345m	1343sh	1338s	$\omega(CH_2)$
1325w		1318w	$\omega(CH_2)$
1232vw			$\tau(CH_2)$
1211w			$\tau(CH_2)$
	1145w	1141w	$\omega(CH_3)$
		1105vw	$\omega(CH_3) + \tau(NH_2)$
1081m		1079vw	$\nu_6(HCOO) + \tau(NH_2)$
1068m		1070vw	$\nu_6(HCOO) + \tau(NH_2)$
	1052m	1056m	$\nu_6(HCOO) + \nu(CNC)$
		1031vw	$\nu(CNC) + \nu(NCC)$
1017m		1020vw	$\nu(CC) + \nu(CNC) + \nu(NCC)$

981m		980vw	$\nu(CC) + \rho(CH_2)$
	919b,w	924vw	$\rho(NH_2)$
	805s	811s, 809s	$\nu_3(HCOO)$
802m	801sh	803s	$\nu_3(HCOO)$
797m		799sh	$\nu_3(HCOO)$
	778m	777m	$\omega(NH_2)$
392w			$\tau(CNC) + \delta(NCC)$
341w			$\delta(NCC) + \tau(CH_3)$
253vw			T'(HCOO)
207vs			L(HCOO)
176vs			L(HCOO)
158sh			L(HCOO)
125sh			L(HCOO)
109sh			$T'(Zn^{2+})$

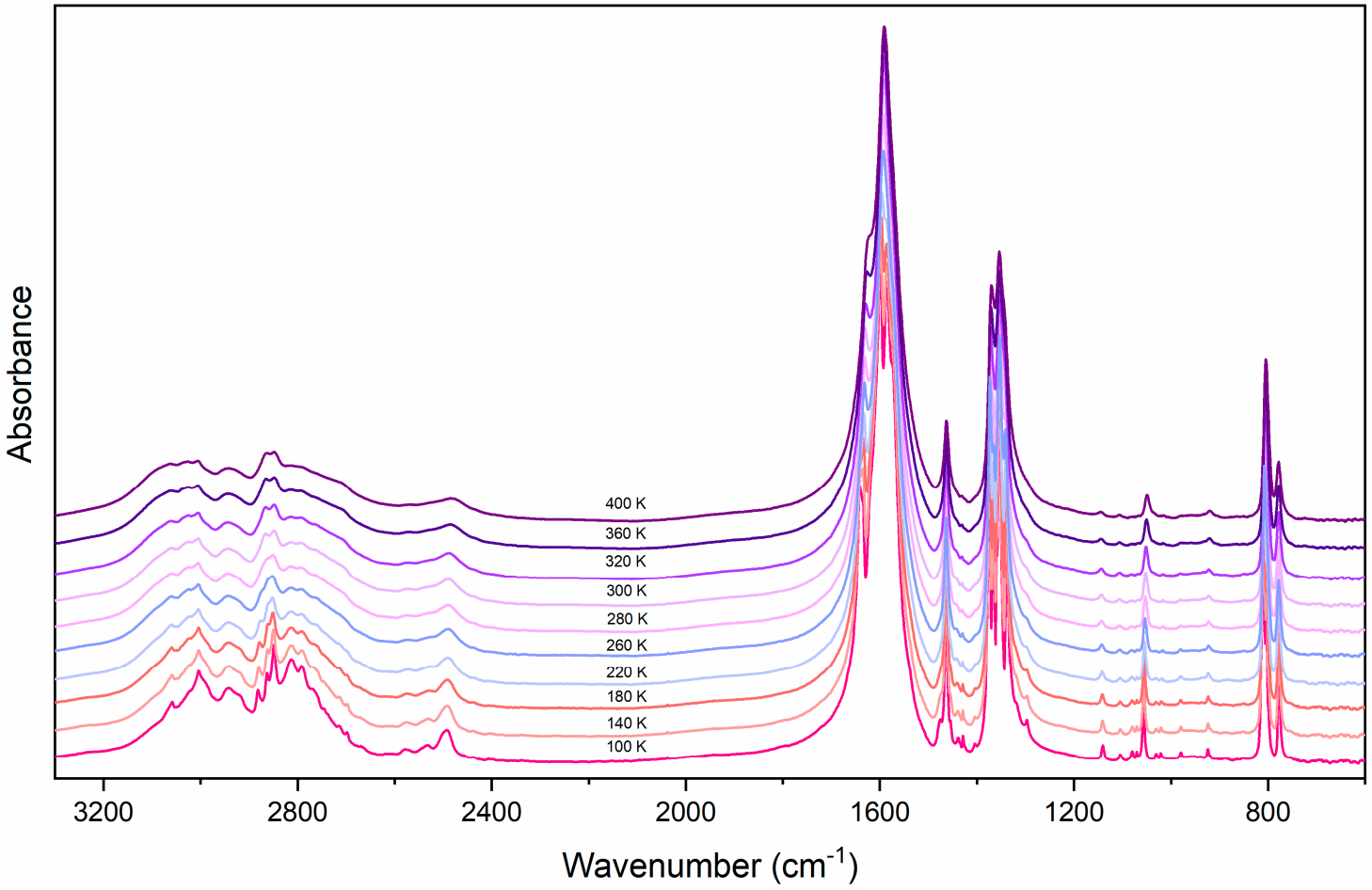

Figure S5. The temperature-dependent IR spectra of the dmenH_2-Zn